

# Wall correction factors, $P_{\text{wall}}$ , for parallel-plate ionization chambers

Lesley A. Buckley<sup>a)</sup> and D. W. O. Rogers<sup>b)</sup>

Ottawa-Carleton Institute of Physics, Carleton University, Ottawa, K1S 5B6 Canada

(Received 29 September 2005; revised 20 January 2006; accepted for publication 5 April 2006; published 24 May 2006)

The EGSnrc Monte Carlo user-code CSnrc is used to calculate wall correction factors,  $P_{\text{wall}}$ , for parallel-plate ionization chambers in photon and electron beams. A set of  $P_{\text{wall}}$  values, computed at the reference depth in water, is presented for several commonly used parallel-plate chambers. These values differ from the standard assumption of unity used by dosimetry protocols by up to 1.7% for clinical electron beams. Calculations also show that  $P_{\text{wall}}$  is strongly dependent on the depth of measurement and can vary by as much as 6% for a 6 MeV beam in moving from a depth of  $d_{\text{ref}}$  to a depth of  $R_{50}$ . In photon beams, where there is limited information available regarding  $P_{\text{wall}}$  for parallel-plate chambers, CSnrc calculations show  $P_{\text{wall}}$  values of up to 2.4% at the reference depth over a range of photon energies. The  $P_{\text{wall}}$  values for photon beams are in good agreement with previous estimates of the wall correction but have much lower statistical uncertainties and cover a wider range of photon beam energies. © 2006 American Association of Physicists in Medicine. [DOI: 10.1118/1.2199988]

Key words: Monte Carlo, dosimetry, correction factor

## I. INTRODUCTION

Current dosimetry protocols<sup>1,2</sup> use calibration coefficients based upon absorbed dose to water standards and rely upon the use of ion chambers for clinical beam calibrations. These protocols use several correction factors in order to relate the measured response of the ion chamber to the absorbed dose to water. The correction factors must account for the presence of the chamber within the phantom in order to determine the absorbed dose to water in the absence of the chamber.

Parallel-plate ion chambers are recommended for use in electron beams, particularly for low-energy electrons. They are suitable for photon beam reference dosimetry only if an absorbed dose to water calibration factor is available for the beam quality of interest. Otherwise, parallel-plate chambers are not recommended for use in photon beams since there is a lack of information regarding the wall corrections for these chambers at photon energies other than  $^{60}\text{Co}$ . One of the primary advantages of parallel-plate ion chambers is their good depth resolution, making them well suited to measurements in high dose gradient regions or in situations where the uncertainty in the point of measurement must be minimized.

The present study investigates the wall correction factor for parallel-plate chambers in high-energy photon and electron beams. The wall correction accounts for the fact that the chamber wall is of a different material from the surrounding phantom material. Unlike cylindrical chambers, where the chamber wall is typically homogeneous, parallel-plate chambers are often constructed such that the chamber walls are composed of several different materials. This has prevented the development of a theory to calculate the wall effect, whereas for cylindrical chambers the Almond-Svensson formalism<sup>3</sup> has been used despite indications that it may not correctly predict the wall correction factor.<sup>4-9</sup> The Monte

Carlo calculation of wall correction factors for cylindrical chambers is discussed in detail elsewhere<sup>10</sup> and confirms that the Almond-Svensson formalism is not accurate.

Measurements of the wall correction factor are, in general, very difficult to perform due to the high degree of precision required and the physical constraints of the chambers. Furthermore, the complexity of the geometry of parallel-plate chambers has, until recent advances in computer power, made a complete Monte Carlo calculation of these factors impractical. The limited information that is available concentrates on electron-beam dosimetry and is often specified in terms of the mean energy at depth and is measured at  $d_{\text{max}}$  rather than the current reference depth,  $d_{\text{ref}}$ . Despite indications that the wall correction alone may be greater than 1%,<sup>6,7,11</sup> both the AAPM's TG-51 protocol<sup>1</sup> and the IAEA's TRS-398 code of practice<sup>2</sup> use a wall correction of unity for parallel-plate chambers in electron beams, citing a lack of available information to make a firm recommendation. Furthermore, neither protocol tabulates data for parallel-plate chambers in photon beams since there is minimal information regarding the corrections for these chambers at photon energies other than  $^{60}\text{Co}$ .

Interest in revisiting the correction factors for parallel-plate chambers is based upon a number of studies that have shown significant corrections in electron beams,<sup>6,7,11</sup> caused primarily by the backscatter from the material behind the air cavity. Hunt *et al.*<sup>6</sup> measured the effect of electron backscatter from materials placed behind the air cavity volume. They measured the effect of electron backscattering as a function of effective atomic number, thickness of the material, and diameter of the backscattering disk. They concluded that most parallel-plate chambers would show a 1–2% effect due to electron backscatter at low electron energies.

A later study by Klevenhagen<sup>7</sup> examined the variation of the electron backscatter as a function of an effective atomic

number in electron beams and proposed an empirical formula to describe this variation. This formula was derived from a fit to measurements using high- $Z$  materials and not the low- $Z$  materials commonly used in chambers for electron-beam dosimetry.

Nilsson *et al.*<sup>11</sup> performed a series of measurements aimed at determining the wall correction factor due to electron backscatter in electron beams. They used a specially designed parallel-plate ion chamber that minimized any perturbation from in-scatter from the side walls, thereby isolating the effects due to the front and back walls only. This chamber allowed them to change the materials on the front and back, as well as the cavity size and therefore they could mimic geometries of commonly used parallel-plate chambers. They also compared their experimental results to Monte Carlo calculations performed using EGS4 the system.<sup>12</sup> They found that in many chamber designs there was an energy-dependent wall correction factor, on the order of 2% at low electron energies.

A preliminary study by Ma and Rogers using the system<sup>13</sup> calculated  $P_{\text{wall}}$  as a function of the electron-beam energy for an NACP and a Markus chamber. Those calculations were performed for a depth of dose maximum,  $d_{\text{max}}$ , in monoenergetic electron beams and showed corrections of up to 1.4% and 2.5% for the NACP and Markus chambers, respectively. They also calculated  $P_{\text{wall}}$  as a function of depth in a water phantom and showed a slight increase in  $P_{\text{wall}}$  with increasing depth.

Williams *et al.*<sup>14</sup> used the EGS4 system to study perturbation factors for the NACP chamber. They calculated an energy-dependent wall correction factor as high as 1.2% for a 4 MeV nominal energy electron beam with an uncertainty on their wall correction factors between 0.21% and 0.47%.

More recently, Sempau *et al.*<sup>15</sup> used the Monte Carlo code PENELOPE<sup>16,17</sup> to study an overall conversion factor for parallel-plate chambers in high-energy electron beams. Rather than determine the individual correction factors, they used a Monte Carlo calculation to compute the total factor required to convert from dose to the cavity to dose to water at the point of interest. This was performed for an NACP chamber and compared to the equivalent values given in the TRS-398 code of practice. They showed that as a function of beam quality, their calculated relative values show similar behavior to the values predicted by the TRS-398 code of practice which assumes  $P_{\text{fl}} = P_{\text{wall}} = 1.00$  in electron beams. Upon normalization to the TRS-398 values, their results showed only minor differences at the lower electron energies. However, this only confirms the variation with energy and not the values in TRS-398, since their paper does not indicate the magnitude of the factor by which the Monte Carlo values were scaled in order to coincide with the TRS-398 values for one high-energy beam. While an overall conversion factor is fundamentally equivalent to the combined effect of the correction factors used in dosimetry, it remains the case that major dosimetry protocols distinguish between the various correction factors for ion chambers and agreement between an overall correction factor and the total correction predicted by the dosimetry protocols does not imply

agreement for any given correction factor. As Sempau *et al.*<sup>15</sup> point out in their paper, this does not matter if one only uses an overall conversion.

In photon beams, Wittkämper *et al.*<sup>18</sup> measured  $P_{\text{wall}}$  values in high-energy photon beams for the NACP and Markus chambers. They used beams with nominal energies ranging from  $^{60}\text{Co}$  to 24 MV. For the NACP chamber, they measured a  $P_{\text{wall}}$  correction of 1.013 in a  $^{60}\text{Co}$  beam, and for the Markus chamber found a  $P_{\text{wall}}$  value of 1.004 for the same beam. For both chambers,  $P_{\text{wall}}$  varied by up to 0.4% over the range of photon beams used in their experiment. The uncertainty on their measured  $P_{\text{wall}}$  values was on the order of  $\pm 0.5\%$ .

In a more recent study, Mainegra *et al.*<sup>19</sup> used the EGSnrc code to calculate  $P_{\text{wall}}$  values for parallel-plate chambers in a  $^{60}\text{Co}$  beam. They too showed nonunity  $P_{\text{wall}}$  values for these chambers. They calculated  $P_{\text{wall}}$  values of 1.0207, 1.0048, and 1.0090 for the NACP, Markus, and Roos chambers, respectively. Their results had statistical uncertainties of less than 0.06%. Their values agree well with other reported  $P_{\text{wall}}$  values for these chambers in  $^{60}\text{Co}$  beams,<sup>20,21</sup> but do show some small systematic differences from earlier EGS4 calculated values<sup>22</sup> which are used in protocols.<sup>1,2</sup>

In light of the lack of conclusive information regarding correction factors for parallel-plate chambers, and due to evidence suggesting that the currently used values are inaccurate, it is useful to revisit some of these correction factors. The present study uses the EGSnrc Monte Carlo code system<sup>23,24</sup> to compute the wall correction factor for a number of commonly used parallel-plate ionization chambers in both photon and electron beams. EGSnrc has been shown to be able to simulate ion chamber response with an accuracy of 0.1% with respect to its own cross sections.<sup>25,26</sup> The calculations are performed using the user-code CSnrc, recently developed for the EGSnrc system to use a correlated sampling variance reduction technique.<sup>27</sup>

## II. THEORY

Clinical dosimetry protocols for electron and photon beams are based upon the Spencer-Attix cavity theory. In this formulation, the dose to the water,  $D_{\text{med}}$ , is related to the dose to the cavity gas,  $D_{\text{gas}}$ , by the restricted stopping-power ratio,  $(\bar{L}/\rho)$ . Assuming that the chamber and the cavity do not perturb the electron spectrum, this relationship is given by

$$D_{\text{med}} = D_{\text{gas}} \left( \frac{\bar{L}}{\rho} \right)_{\text{gas}}^{\text{med}}. \quad (1)$$

For real chambers, the presence of the chamber and the cavity will affect the electron fluence spectrum and, therefore, corrections are required to the Spencer-Attix cavity theory. The absorbed dose to water formalism, with corrections, for a parallel-plate chamber, becomes

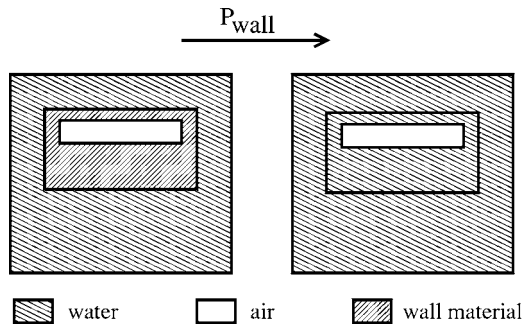


FIG. 1. Schematic showing simplified versions of the two geometries used to compute  $P_{\text{wall}}$ . The CSnrc user-code handles both geometries in a single execution of the code, changing only the materials of the chamber wall during the simulation and allows for multiple different wall materials.  $P_{\text{wall}}$  is computed as the ratio of the dose to the sensitive volume of the cavity in a chamber composed entirely of water to that in a chamber with a detailed model of the realistic chamber wall.

$$D_{\text{med}} = D_{\text{gas}} \left( \frac{\bar{L}}{\rho} \right)_{\text{gas}}^{\text{med}} P_{\text{wall}} P_{\text{repl}}. \quad (2)$$

The wall correction,  $P_{\text{wall}}$ , accounts for the fact that the chamber wall is of a different material than the phantom. The replacement correction,  $P_{\text{repl}}$ , is composed of two components,  $P_{\text{fl}}$  and  $P_{\text{gr}}$ .  $P_{\text{fl}}$  is the fluence correction, and corrects for changes in the electron fluence spectrum due to the presence of the cavity. It results from two main effects: the in-scatter effect which increases the fluence in the cavity due to electrons that are scattered into the cavity by the walls and to the fact that electrons are not scattered out by the gas and the obliquity effect which decreases the fluence since electrons go straight instead of scattering in the cavity. For many parallel-plate chambers,  $P_{\text{fl}}$  is assumed to be unity, but is taken to have nonunity values for chambers which are not well guarded.<sup>28</sup>  $P_{\text{gr}}$  is the gradient correction which accounts for the shift upstream of the effective point of measurement of the ion chamber due to the cavity. For parallel-plate cham-

bers,  $P_{\text{gr}}$  is taken as unity when the point of measurement is at the front of the air cavity. Parallel-plate chambers do not have a central electrode, and therefore the electrode correction,  $P_{\text{cel}}$ , used for cylindrical chambers, is not required.

The values of  $P_{\text{wall}}$  and  $P_{\text{repl}}$  are integral to the computation of the beam quality conversion factor,  $k_Q$ , which is required for each chamber in order to convert from a calibration coefficient in a  $^{60}\text{Co}$  beam to that in the beam quality of interest. The quantity  $k_Q$  is defined by

$$N_{D,w}^Q = k_Q N_{D,w}^{60\text{Co}}, \quad (3)$$

where  $N_{D,w}^Q$  is the absorbed dose to water calibration coefficient for a beam quality  $Q$ . For many chambers,  $k_Q$  is provided within the dosimetry protocol, but it may also be computed for photon beams using<sup>29</sup>

$$k_Q = \frac{\left[ \left( \frac{\bar{L}}{\rho} \right)_{\text{air}}^w P_{\text{wall}} P_{\text{repl}} \right]_Q}{\left[ \left( \frac{\bar{L}}{\rho} \right)_{\text{air}}^w P_{\text{wall}} P_{\text{repl}} \right]_{60\text{Co}}}. \quad (4)$$

For electron beams,  $k_Q$  has two components:<sup>30</sup>  $k_Q = k_{R_{50}} P_{\text{gr}}$ , where  $P_{\text{gr}}$  is taken as unity for parallel-plate chambers and  $k_{R_{50}}$  is given by

$$k_{R_{50}} = \frac{\left[ \left( \frac{\bar{L}}{\rho} \right)_{\text{air}}^w P_{\text{wall}} P_{\text{fl}} \right]_{R_{50}}}{\left[ \left( \frac{\bar{L}}{\rho} \right)_{\text{air}}^w P_{\text{wall}} P_{\text{fl}} P_{\text{gr}} \right]_{60\text{Co}}}. \quad (5)$$

Problems with the values of the correction factors will therefore affect the value of  $k_Q$  or  $k_{R_{50}}$  and, in turn, will influence the calibration coefficients for the user's beam.

### III. MONTE CARLO CALCULATIONS

The values of  $P_{\text{wall}}$  are computed using the EGSnrc user-code, CSnrc. CSnrc uses correlated sampling as a variance reduction technique and can simulate a cylindrical chamber in a rectangular phantom. The details of the correlated sam-

TABLE I. Details of the chamber geometries for the parallel-plate chambers studied here.

Chamber	Materials	Window thickness (mg/cm <sup>2</sup> )	Electrode diameter (mm)	Guard ring width (mm)
NACP-02	Graphited rexolite electrodes and housing, graphite body, mylar foil and graphite window	104	10	3
Roos	PMMA, graphited electrodes	118	16	4
Markus	Graphited polyethylene foil, graphited polystyrene collector, PMMA body	0.42	5.3	0.2
Capintec PS-033	Aluminized mylar foil window, air equivalent electrode, polystyrene body	0.5	16.2	2.5

TABLE II. Details of the input spectra used for the  $P_{\text{wall}}$  calculations. For photon beams, the nominal beam energy is shown along with the beam quality specifiers  $\%dd(10)_x$  and the  $TPR_{10}^{20}$ . For electron beams, the nominal energy is shown along with  $R_{50}$  and the reference depth for each beam. The input spectra were taken from previously published works.<sup>a</sup>

Photon beams			
Description	$E_{\text{nominal}}$ (MV)	$\%dd(10)_x$ <sup>b</sup>	$TPR_{10}^{20}$ <sup>b</sup>
Eldorado 6 <sup>60</sup> Co	-	58.3	0.571
Varian Clinac	4	62.7	0.616
	6	66.5	0.658
	10	73.8	0.728
	15	77.7	0.750
	18	81.3	0.774
Elekta SL25	25	82.7	0.786
Electron beams			
Description	$E_{\text{nominal}}$ (MeV)	$R_{50}$ (cm) <sup>c</sup>	$d_{\text{ref}}$ (cm)
Varian Clinac	6	2.63	1.48
	9	4.00	2.30
	12	5.20	3.01
	15	6.50	3.80
	18	7.72	4.53
Therac 20	6	2.18	1.21
	9	3.42	1.95
	20	8.10	4.76
Philips SL75-20	5	2.08	1.15
Siemens KD2	21	8.30	4.88
Racetrack MM50	25	10.36	6.12

<sup>a</sup>See Refs. 33–35.

<sup>b</sup>Taken from Kalach and Rogers—Ref. 37.

<sup>c</sup>Taken from Ding and Rogers—Ref. 35.

pling technique as it is implemented in CSnrc are described elsewhere.<sup>27</sup> For the present calculations, CSnrc improves the efficiency by a factor of 3–4 over using the EGSnrc user-code CAVRZnrc.<sup>31</sup>

Figure 1 shows a schematic representation of how the calculation geometries are arranged to compute the  $P_{\text{wall}}$  correction factor. CSnrc computes the ratio of the dose to the sensitive volume in the air cavity for a chamber wall composed entirely of water to that for a real chamber geometry. Both geometries shown in Fig. 1 are simulated in a single execution of the CSnrc code. For simplicity, the chamber wall is shown as a single region in Fig. 1, but in the CSnrc calculations, detailed chamber geometries are used. Table I outlines some of the details of the chamber geometries. The CSnrc input files used here are adapted from a previous EGSnrc study of parallel-plate chambers by Mainegra *et al.*<sup>19</sup>

CSnrc is also used to calculate the ratio of the dose to water at the point of measurement to the dose to the sensitive volume of the air cavity. The dose to the sensitive region in the chamber is taken from the  $P_{\text{wall}}$  calculations described above. The dose to the water is calculated for a thin slab, 0.1 mm thick, with a front face at a depth in water equal to

the point of measurement for the chamber. The radius of the scoring region is equal to the radius of the sensitive volume of the chamber.

For all of the in-phantom simulations, the ionization chamber is placed in a  $30 \times 30 \times 30$  cm<sup>3</sup> water phantom. The chamber is placed at the reference depth in water, as defined by the TG-51 protocol:<sup>1</sup> 10 cm for photon beams, and at  $d_{\text{ref}} = 0.6R_{50} - 0.1$  cm for electron beams, where  $R_{50}$ , expressed in centimeters, is the beam quality specifier for the electron beam. As specified by the protocol, the point of measurement of the parallel-plate chambers is taken to be the front face of the air cavity. For all calculations, there is a  $10 \times 10$  cm<sup>2</sup> field incident on the phantom. The electron cut-off energy,  $AE$ , is 521 keV and the photon cutoff energy,  $AP$ , is 10 keV. Calculations show that the largest change in  $P_{\text{wall}}$  due to a change in the value of  $AE$  from 521 keV to 512 keV is 0.3% and is in most cases much smaller. An earlier study in a <sup>60</sup>Co beam<sup>19</sup> showed that for the chambers considered here, this effect was less than 0.16%. Varying the value of  $AP$  does not significantly impact the value of  $P_{\text{wall}}$  in the present calculations. Photon splitting,<sup>31,32</sup> with a splitting factor of 160, is used in all calculations and improves the efficiency by a factor of about 3. Multiple scattering spin effects<sup>23,24</sup> are turned on. The incident photon spectra include a <sup>60</sup>Co spectrum<sup>33</sup> and several higher-energy photon spectra<sup>34</sup> previously published. The incident electron-beam spectra are taken from the work of Ding and Rogers.<sup>35</sup> The details of all of the input spectra are presented in Table II.

## IV. RESULTS

### A. Values of $P_{\text{wall}}$ in electron beams

#### 1. $P_{\text{wall}}$ values for several commonly used ion chambers

Current dosimetry protocols assume a value of unity for  $P_{\text{wall}}$  in electron beams due to insufficient evidence upon which to base the adoption of nonunity values. This is despite experimental and Monte Carlo evidence, described previously, that indicates a nonunity  $P_{\text{wall}}$  correction for some chambers. For this reason, it is useful to present here a complete set of calculated values of  $P_{\text{wall}}$  for a series of commonly used parallel-plate ionization chambers. We have presented similar calculated  $P_{\text{wall}}$  values elsewhere for cylindrical chambers.<sup>10</sup>

Figure 2 shows  $P_{\text{wall}}$  as a function of  $R_{50}$  for the NACP chamber. The nominal energies in Fig. 2 range from 5 MeV to 21 MeV, and all values are calculated at the reference depth in water. The scatter in the values is typical of all of the chambers studied in the present work. Also shown is a linear fit to the values calculated using CSnrc. Figure 2 shows that  $P_{\text{wall}}$  for the NACP chamber varies from 1.017 near  $R_{50} = 2.1$  cm to 1.008 near  $R_{50} = 8.3$  cm. This size of  $P_{\text{wall}}$  correction is similar to that estimated by Nilsson *et al.*<sup>11</sup> who considered the effect of the front and back walls of the NACP chamber in a polymethylmethacrylate (PMMA) phantom which, of course, is not equivalent to  $P_{\text{wall}}$  in a water phantom. The CSnrc results are also in reasonable agreement

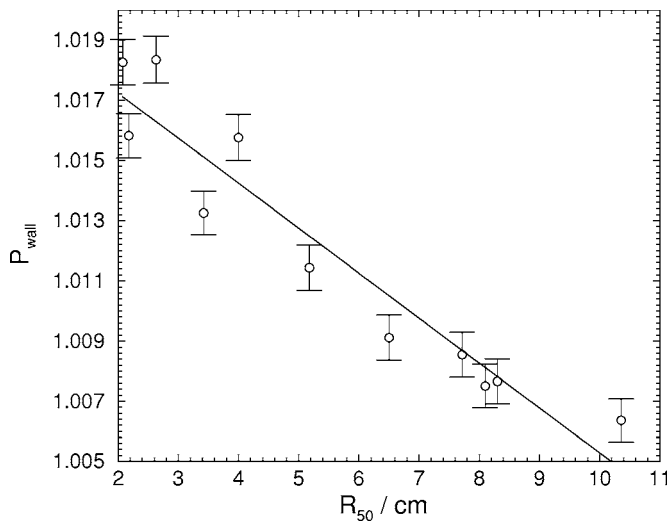


FIG. 2. Calculated  $P_{\text{wall}}$  values at  $d_{\text{ref}}$  as a function of the beam quality,  $R_{50}$ , for an NACP chamber in a water phantom irradiated by a  $10 \times 10 \text{ cm}^2$  beam. The solid line shows a linear fit to the CSnrc-calculated values. The calculated  $P_{\text{wall}}$  values are in contrast to the  $P_{\text{wall}}$  of unity used in current dosimetry practice.

with a previous study by Ma and Rogers<sup>13</sup> that found  $P_{\text{wall}}$  values for the NACP chamber at  $d_{\text{max}}$  varying from 1.014 to 0.999 for monoenergetic electron beams in the range of 4 MeV to 20 MeV. The statistical uncertainties of their results were on the order of 0.4% compared to 0.1% in the present calculations. The variation of the CSnrc values of  $P_{\text{wall}}$  over the range of  $R_{50}$  values considered here is slightly greater than in another earlier Monte Carlo study, which had considerably poorer statistics. In that case, Williams *et al.*<sup>14</sup> found that, over a range of nominal energies from 4 MeV to 19 MeV,  $P_{\text{wall}}$  varied from  $1.0127 \pm 0.21\%$  to  $1.0065 \pm 0.47\%$ , again at  $d_{\text{max}}$ . The present values of  $P_{\text{wall}}$  are about 0.5% larger at low energies. We believe the current values are more reliable since EGSnrc is considerably more accurate than when calculating ion chamber response.

The other parallel-plate chambers studied here show similar trends in the  $P_{\text{wall}}$  values as a function of  $R_{50}$ . Figure 3 shows  $P_{\text{wall}}$  values for each of the chambers included in this study. The straight lines are fit lines to the CSnrc-calculated  $P_{\text{wall}}$  values for each chamber. All chambers show a  $P_{\text{wall}}$  correction on the order or 1% or larger at the lower-energy beams. In all cases, this correction decreases as a function of  $R_{50}$  and varies by 1% or more over a range of nominal energies from 5 MeV to 25 MeV. The scatter of points was typically  $\pm 0.2\%$  about the fit line.<sup>38</sup> This scatter is in part due to differences in beam quality. The Therac beams are swept beams, and are consequently much more monoenergetic. They show consistently lower values of  $P_{\text{wall}}$  than the neighboring points from scattering foil accelerators. When the same calculations are repeated using monoenergetic electron beams,  $P_{\text{wall}}$  varies more smoothly as a function of  $R_{50}$ . This suggests that  $P_{\text{wall}}$  is affected by the type of beam, and therefore that  $R_{50}$  does not adequately describe the beam quality for  $P_{\text{wall}}$  calculations.

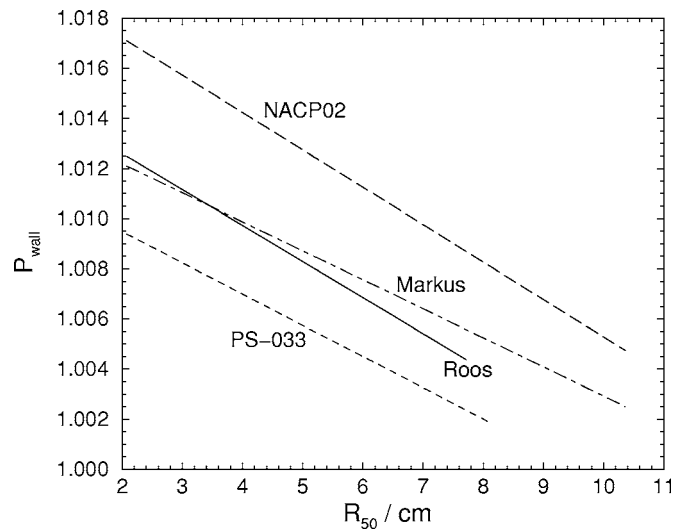


FIG. 3.  $P_{\text{wall}}$  as a function of  $R_{50}$  for several commonly used parallel-plate ion chambers with the calculation details as per Fig. 2. The lines are linear fits to the calculated  $P_{\text{wall}}$  values for the beam qualities described in Table II. The scatter about the fit lines is on the order of  $\pm 0.2\%$  and is shown for the NACP chamber in Fig. 2.

## 2. $P_{\text{wall}}$ as a function of depth of measurement

In electron beams, ion chamber measurements are very sensitive to the depth of measurement within the water phantom. CSnrc is used to investigate the sensitivity of  $P_{\text{wall}}$  to the depth of measurement. The calculations are performed for an NACP chamber in both a 6 MeV and a 20 MeV beam, and the depths are varied from much less than  $d_{\text{ref}}$  to a depth of nearly  $R_{50}$  for each beam. Figure 4 shows that for the 6 MeV beam there is a striking variation in  $P_{\text{wall}}$  with depth. For this beam, there is a 5% variation in  $P_{\text{wall}}$  between  $d_{\text{ref}}$  and  $R_{50}$ . For the 20 MeV beam, this variation is less, at

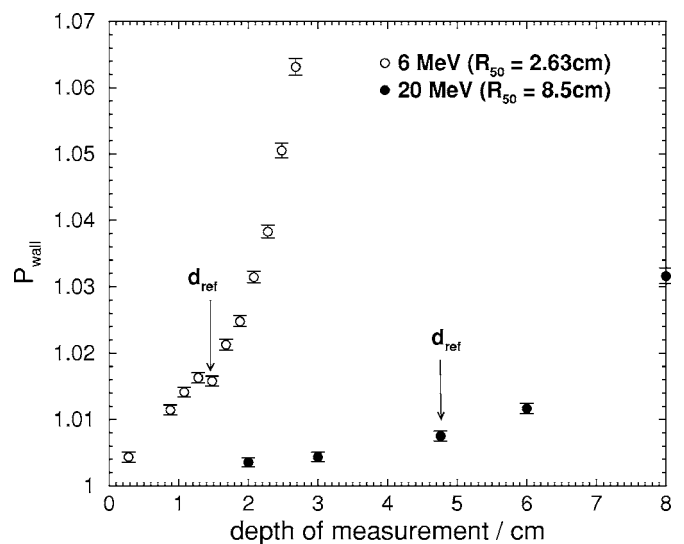


FIG. 4.  $P_{\text{wall}}$  as a function of depth of measurement for an NACP chamber in a water phantom. The calculations were performed using the CSnrc user-code for nominal beam energies of 6 MeV and 20 MeV. The reference depths for each beam,  $d_{\text{ref}}$ , specified by the standard dosimetry protocols, are indicated by the arrows.

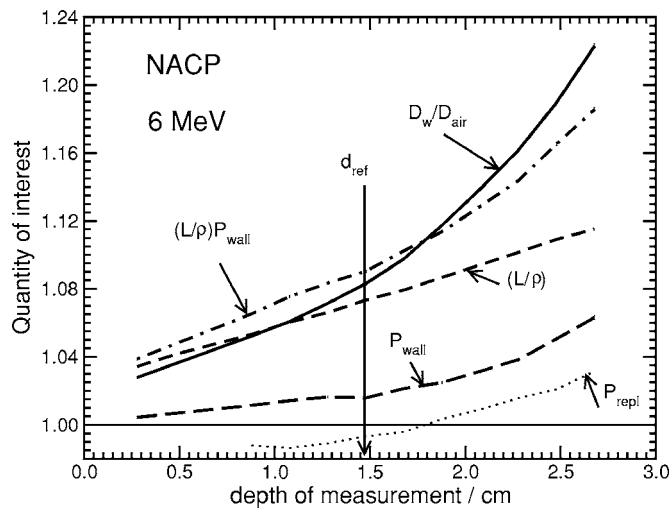


Fig. 5. CSnrc calculations for an NACP chamber of several of the factors involved in the dosimetry formalism employed in TG-51 as a function of depth of measurement in a Varian 6 MeV electron beam ( $R_{50}=2.63$  cm). For a parallel-plate chamber in electron beams, the protocol predicts that the ratio of doses,  $D_{\text{water}}/D_{\text{air}}$  should equal the stopping power ratio of water to air. Also shown is the variation in  $P_{\text{wall}}$  calculated using CSnrc. The product  $(\bar{L}/\rho)_{\text{air}}^{\text{water}} P_{\text{wall}}$  shows better agreement with the dose ratios than the simple stopping power ratio, consistent with a nonunity  $P_{\text{wall}}$  correction factor for the NACP chamber. The  $P_{\text{repl}}$  curve shows the deviation between the dose ratio and the product of the stopping-power and  $P_{\text{wall}}$ .

2.3%, but significant nonetheless. This variation with depth is not simply due to the difference in density of the front wall. If this were the case, the added density of the front wall would correspond to a shift in the effective depth of the chamber and in the region of nearly linear dose falloff of the depth-dose curve, this would result in a constant value of  $P_{\text{wall}}$ , which is not the case.

The magnitude of the variation in  $P_{\text{wall}}$  with depth is somewhat surprising given that such a drastic departure from standard dosimetry theory has not been seen in practice. If one compares the stopping-power ratio at depth to the ratio of the dose to water to the dose to the air in the chamber cavity [Eq. (2)], standard dosimetry formalism suggests that these quantities have the same value since the correction factors in Eq. (2) are traditionally taken to be unity for the NACP chamber. However, as shown in Fig. 5 for a 6 MeV beam, when calculated using CSnrc the stopping-power ratio curve and the ratio of doses diverge as the depth considered is increased. If the current  $P_{\text{wall}}$  values are used as a correction to the standard dosimetry theory, the product  $(\bar{L}/\rho)_{\text{air}}^{\text{water}} P_{\text{wall}}$  shows much better agreement with the dose ratios. This is also true in the case of the 20 MeV beam, where the product  $(\bar{L}/\rho)_{\text{air}}^{\text{water}} P_{\text{wall}}$  lies on top of the dose ratio curve and there is only a noticeable difference between the two curves for depths beyond 6 cm.<sup>38</sup> Differences between the  $(\bar{L}/\rho)_{\text{air}}^{\text{water}} P_{\text{wall}}$  curve and the stopping-power ratio curve may be attributed to the replacement correction,  $P_{\text{repl}}$ . In other words, we can calculate  $P_{\text{repl}}$  as  $(D_w/D_{\text{air}})/((\bar{L}/\rho)P_{\text{wall}})$ . The behavior of  $P_{\text{repl}}$  seen in Fig. 5 agrees qualitatively with re-

sults of Ma and Nahum<sup>36</sup> who showed that  $P_{\text{repl}}$  increased with increasing depth for an NACP chamber in monoenergetic electron beams.

### 3. Comparison to overall correction calculations

In a recent study, Sempau *et al.*<sup>15</sup> calculated an overall correction factor to be used in Eq. (2). They computed the ratio of the dose to water at the point of measurement of an NACP chamber for a geometry composed entirely of water to the dose to air for a realistic NACP chamber at depth in a water phantom. Their results were presented as an overall chamber correction factor, as a function of beam quality. In the notation employed in Eq. (2), their correction factor corresponds to the product  $(\bar{L}/\rho)_{\text{gas}}^{\text{med}} P_{\text{wall}} P_{\text{repl}}$ . They concluded that there was no significant discrepancy between their calculations and the predictions of the IAEA's TRS-398 code of practice,<sup>2</sup> which, like the TG-51 protocol,<sup>1</sup> assumes values of unity for both  $P_{\text{repl}}$  and  $P_{\text{wall}}$  for the NACP chamber and uses the same stopping powers. With the correction factors assumed to be unity, both TRS-398 and TG-51 predict that the ratio of the dose to water to the dose to the cavity should equal the stopping power ratio. Sempau *et al.*<sup>15</sup> concluded that there were only some small deviations at lower electron energies between their calculations and the predictions of the dosimetry protocols.

The present results from CSnrc for  $P_{\text{wall}}$  values in electron beams show a nonunity  $P_{\text{wall}}$  factor and are seemingly in conflict with the results of Sempau *et al.*<sup>15</sup> In some cases, the calculated  $P_{\text{wall}}$  value is as high as 2%. This magnitude of correction was not indicated in the study by Sempau *et al.* The difficulty in comparing the two sets of calculations is that the results of Sempau *et al.*<sup>15</sup> were normalized by an unspecified amount in order to give agreement with the TRS-398 values at  $R_{50}=8.75$  cm. Furthermore, it is possible that the replacement correction  $P_{\text{repl}}$  may offset the  $P_{\text{wall}}$  correction, leading to a smaller overall change compared to the standard theory than the individual  $P_{\text{wall}}$  values indicate.

In order to investigate the issue of the normalization of the Sempau *et al.*<sup>15</sup> results, CSnrc is used to repeat the calculations of the overall correction factor as in Fig. 5. For these calculations, the NACP chamber is placed at the reference depth in water for each electron beam used. The ratio of the dose to water to the dose to air is calculated at each beam quality and is presented in Fig. 6. The CSnrc results are shown without normalization alongside the identical TRS-398 and TG-51 prediction and the normalized results of Sempau *et al.*<sup>15</sup> In their paper, Sempau *et al.*<sup>15</sup> normalized the values to the TRS-398 value at  $R_{50}=8.75$  cm. For the present study, the CSnrc calculated values were normalized to the TRS-398 value at  $R_{50}=8.3$  cm, as this was the CSnrc point closest to the Sempau *et al.*<sup>15</sup> point of normalization. The normalized values from CSnrc are also presented in Fig. 6. The statistical uncertainty on the CSnrc values is on the order of 0.06% and the normalization factor is 0.9926.

Figure 6 shows that the current overall dose ratio results, once normalized agree with the previously published results of Sempau *et al.*<sup>15</sup> As in the case of their results, if the

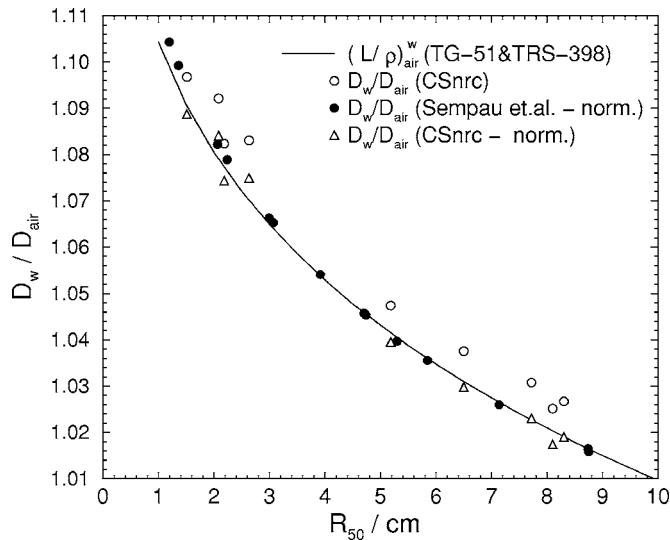


FIG. 6. The overall correction factor for an NACP chamber in electron beams as a function of beam quality. The CSnrc values ( $\circ$ ) show the ratio of dose to water at the point of measurement to dose to air in the NACP chamber. The dose ratios are shown in comparison to the predicted values of the TRS-398 code of practice (Ref. 2) and the previously published calculations of Sempau *et al.* (Ref. 15). The values from Sempau *et al.* are taken from digitization of Fig. 2 of their paper. The CSnrc values are also shown, normalized to the TRS-398 point at  $R_{50}=8.3$  cm ( $\Delta$ ). The statistical uncertainties on the CSnrc values are on the order of 0.06%.

present values are normalized to a TRS-398 point for large  $R_{50}$ , the calculated data show the same shape as the stopping power ratio curve with slight fluctuations around it. Since the study by Sempau *et al.*<sup>15</sup> was conducted entirely at a measurement depth of  $d_{\text{ref}}$ , the larger discrepancies between the calculations and the standard theory at deeper depths did not affect the comparison. While the normalized curve and the stopping-power ratio curve show the same behavior as a function of beam quality, the need for a normalization suggests an overall correction of 1.0074, not unity as predicted by TRS-398 and TG-51. This correction is smaller than the  $P_{\text{wall}}$  values presented earlier, suggesting that the replacement correction must behave in a way to cancel some of the wall effects. So although Fig. 2 shows a wall correction of 1.8% for the 6 MeV beam ( $R_{50}=2.63$  cm), in Fig. 6 the discrepancy between the nonnormalized point and the stopping power ratio curve is only 1.2%. At  $d_{\text{ref}}$  in Fig. 5,  $P_{\text{repl}}$  has a value of 0.994 which would partially offset the  $P_{\text{wall}}$  value. Despite this partial offset, our values of  $D_w/D_{\text{air}}$  show a 1.2% discrepancy with the values used by TG-51/TRS-398. This is markedly different from the impression given in the Sempau *et al.* paper.<sup>15</sup>

## B. $P_{\text{wall}}$ values in photon beams

Parallel-plate chambers are less commonly used in high-energy photon beams than in electron beams, in part due to the lack of information regarding the correction factors for these chambers in photon beams. Figure 7 shows the wall correction  $P_{\text{wall}}$  as a function of photon beam quality for several commonly used parallel-plate chambers at 10 cm depth in  $10 \times 10$  cm<sup>2</sup> beams. As in the case of electron

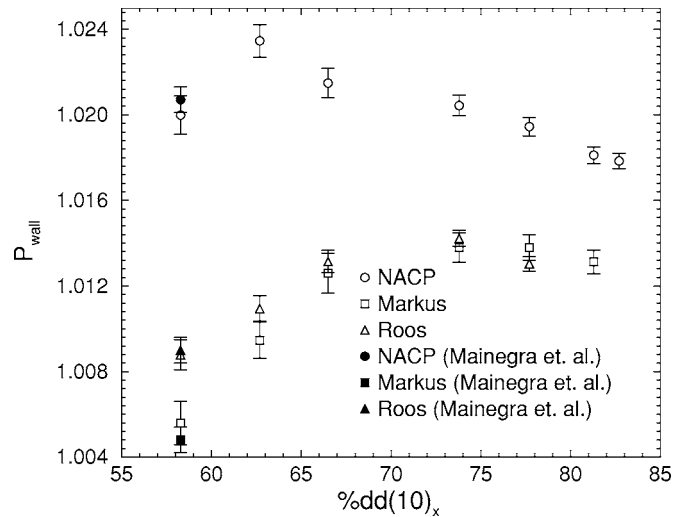


FIG. 7.  $P_{\text{wall}}$  as a function of  $\%dd(10)_x$  for several parallel-plate chambers in high-energy photon beams. Also shown are previously calculated values of  $P_{\text{wall}}$  in a  $^{60}\text{Co}$  beam from Mainegra *et al.* (Ref. 19).

beams, these chambers show a significant wall correction. Also shown in Fig. 7 are previously calculated values of  $P_{\text{wall}}$  in  $^{60}\text{Co}$  beams from Mainegra *et al.*<sup>19</sup> The present results are in good agreement with the results from Mainegra *et al.*<sup>19</sup> which were shown to agree with measured values (which have a large scatter and large uncertainty).

Compared to previous experimental results from Wittkämper *et al.*, the CSnrc values of  $P_{\text{wall}}$  are higher by up to 1%. It is possible that the discrepancy between the Monte Carlo results and the Wittkämper *et al.*<sup>18</sup> results is due to the added uncertainty in their values due to the measurement technique. In order to determine  $P_{\text{wall}}$  for the parallel-plate chambers, they compared measurements using the parallel-plate chambers to measurements made with a reference cylindrical chamber for which they assumed the correction factors were well known. Their stated uncertainty of 0.6% does not include uncertainties in the  $P_{\text{wall}}$ ,  $P_{\text{cel}}$ , or  $P_{\text{fl}}$  values for the cylindrical chamber. Previous calculations<sup>10,27</sup> show that there are potentially significant errors in the standard values for these correction factors. If recent values of  $P_{\text{wall}}$ <sup>10</sup> for the reference cylindrical chamber are used instead of the values from the Almond-Svensson formalism as was used in the Wittkämper *et al.*<sup>18</sup> paper, their  $P_{\text{wall}}$  values change for the Markus and NACP chambers. These corrected  $P_{\text{wall}}$  values show much closer agreement with the current CSnrc set of  $P_{\text{wall}}$  values.

## V. CONCLUSIONS

The EGSnrc user-code CSnrc has been used to compute the wall correction factor  $P_{\text{wall}}$  for parallel-plate ionization chambers. CSnrc uses a correlated sampling variance reduction technique to achieve greater calculation efficiency and yields lower statistical uncertainties than previously published values of  $P_{\text{wall}}$ . The CSnrc calculations agree well with earlier Monte Carlo studies and with experimental estimates of the magnitude of the wall effect.

A set of  $P_{\text{wall}}$  values has been presented for four commonly used parallel-plate chambers in high-energy electron beams. The calculations were performed consistently, with the chamber placed at the TG-51 reference depth in a  $30 \times 30 \times 30 \text{ cm}^3$  water phantom. When compared to the assumptions of the standard dosimetry protocols, which use  $P_{\text{wall}}$  values of unity in electron beams, the present set of  $P_{\text{wall}}$  values show corrections as large as 1.7%. The CSnrc calculations show that  $P_{\text{wall}}$  has a strong dependence on the depth of measurement and the value of  $P_{\text{wall}}$  for an NACP chamber in a 6 MeV beam varies by 5% in going from a depth of  $d_{\text{ref}}$  to a depth of  $R_{50}$ . When an overall correction factor is computed for the NACP chamber at  $d_{\text{ref}}$ , on average, the overall correction is 1.0074, with corrections up to 1.2% necessary. This is in contrast to the impression given by Sempau *et al.*<sup>15</sup> that the overall correction is 1.0, as used in the TG-51 and TRS-398 protocols. Our results indicate that at the reference depth, the effects of  $P_{\text{wall}}$  are in part cancelled by the replacement correction,  $P_{\text{repl}}$ . However, as shown by Fig. 5, at greater depths,  $P_{\text{repl}}$  contributes to the correction needed to the standard approach in TG-51 or TRS-398.

A similar set of calculations for three of the parallel-plate chambers in high-energy photon beams also show large  $P_{\text{wall}}$  corrections. For these calculations, the chambers were placed at a depth of 10 cm in a water phantom. The CSnrc values of  $P_{\text{wall}}$  agree well with previously calculated results from Mainegra *et al.*<sup>19</sup> in  $^{60}\text{Co}$  beams and show corrections of up to 2.3% in some cases. The new set of  $P_{\text{wall}}$  values are presented for a range of photon beam energies, up to a nominal beam energy of 25 MV and should allow confident use of parallel-plate chambers in photon beams.

The discrepancies between the present calculations and the currently used values in dosimetry protocols indicate the need for changes to the  $P_{\text{wall}}$  values now used, particularly for precise work. Taking these results into account will require the reanalysis of many old experiments, since many analyses have been based on incorrect values of  $P_{\text{wall}}$ . Further work on the replacement correction is needed.

## ACKNOWLEDGMENTS

This work was supported by the Canada Research Chairs program and NSERC. We thank Iwan Kawrakow of the NRC for allowing many of the calculations to be performed on their computing cluster.

<sup>a)</sup> Also at: National Research Council of Canada, Ottawa, ON K1A 0R6 Canada; now at Ottawa Hospital Regional Cancer Centre, Ottawa, ON K1H 1C4, Canada.

<sup>b)</sup> Electronic mail: drogers@physics.carleton.ca

<sup>1</sup> P. R. Almond, P. J. Biggs, B. M. Coursey, W. F. Hanson, M. S. Huq, R. Nath, and D. W. O. Rogers, "AAPM's TG-51 protocol for clinical reference dosimetry of high-energy photon and electron beams," *Med. Phys.* **26**, 1847–1870 (1999).

<sup>2</sup> IAEA, *Absorbed Dose Determination in External Beam Radiotherapy: An International Code of Practice for Dosimetry Based on Standards of Absorbed Dose to Water*, Technical Report Series, Vol. 398 (IAEA, Vienna, 2001).

<sup>3</sup> P. R. Almond and H. Svensson, "Ionization chamber dosimetry for

photon and electron beams," *Acta Radiol.: Ther., Phys., Biol.* **16**, 177–186 (1977).

<sup>4</sup> M. T. Gillin, R. W. Kline, A. Niroomand-Rad, and D. F. Grimm, "The effect of thickness of the waterproofing sheath on the calibration of photon and electron beams," *Med. Phys.* **12**, 234–236 (1985).

<sup>5</sup> W. F. Hanson and J. A. D. Tinoco, "Effects of plastic protective caps on the calibration of therapy beams in water," *Med. Phys.* **12**, 243–248 (1985).

<sup>6</sup> M. A. Hunt, G. J. Kutcher, and A. Buffa, "Electron backscatter correction for parallel-plate chambers," *Med. Phys.* **15**, 96–103 (1988).

<sup>7</sup> S. C. Klevenhagen, "Implications of electron backscatter for electron dosimetry," *Phys. Med. Biol.* **36**, 1013–1018 (1991).

<sup>8</sup> C. K. Ross, K. R. Shortt, D. W. O. Rogers, and F. Delaunay, "A test of TPR<sub>10</sub><sup>20</sup> as a beam quality specifier for high-energy photon beams, IAEA-SM-330/10," in *Proceedings of Symposium on Measurement Assurance in Dosimetry* (IAEA, Vienna, 1994), pp. 309–321.

<sup>9</sup> J. P. Seuntjens, C. K. Ross, K. R. Shortt, and D. W. O. Rogers, "Absorbed-dose beam quality conversion factors for cylindrical chambers in high-energy photon beams," *Med. Phys.* **27**, 2763–2779 (2000).

<sup>10</sup> L. A. Buckley and D. W. O. Rogers, "Wall correction factors,  $P_{\text{wall}}$ , for thimble ionization chambers," *Med. Phys.* **33**, 455–464 (2006).

<sup>11</sup> B. Nilsson, A. Montelius, and P. Andreo, "Wall effects in plane-parallel ionization chambers," *Phys. Med. Biol.* **41**, 609–623 (1996).

<sup>12</sup> W. R. Nelson, H. Hirayama, and D. W. O. Rogers, "The Code System," Report SLAC-265 (Stanford Linear Accelerator Center, Stanford, California, 1985).

<sup>13</sup> C.-M. Ma and D. W. O. Rogers, "Monte Carlo calculated wall correction factors for plane-parallel chambers in high-energy electron beams," *Proceedings of the 1995 COMP Annual Meeting* (Canadian Organization of Medical Physicists, Edmonton, Alberta), (1995), pp. 117–118.

<sup>14</sup> A. J. Williams, M. R. McEwen, and A. R. DuSautoy, "A calculation of the water to graphite perturbation factors for the NACP type02 ionization chamber using Monte Carlo techniques," NPL Report CIRM 13 (NPL, Teddington, UK, 1998).

<sup>15</sup> J. Sempau, P. Andreo, J. Aldana, J. Mazurier, and F. Salvat, "Electron-beam quality correction factors for plane-parallel ionization chambers: Monte Carlo calculations using the PENELOPE system," *Phys. Med. Biol.* **49**, 4427–4444 (2004).

<sup>16</sup> J. Baro, J. Sempau, J. M. Fernandez-Varea, and F. Salvat, "PENELOPE: An algorithm for Monte Carlo simulation of the penetration and energy loss of electrons and positrons in matter," *Nucl. Instrum. Methods Phys. Res. B* **100**, 31–46 (1995).

<sup>17</sup> F. Salvat, J. M. Fernandez-Varea, and J. Sempau, "PENELOPE—A code system for Monte Carlo simulation of electron and photon transport," Technical report (OECD Nuclear Energy Agency, Issy-les-Moulineaux, France, 2003).

<sup>18</sup> F. W. Wittkämper, A. H. L. Aalbers, and B. J. Mijnheer, "Experimental determination of wall correction factors. Part II: NACP and Markus plane-parallel ionization chambers," *Phys. Med. Biol.* **37**, 995–1004 (1992).

<sup>19</sup> E. Mainegra-Hing, I. Kawrakow, and D. W. O. Rogers, "Calculations for plane-parallel ion chambers in  $^{60}\text{Co}$  beams using the EGSnrc Monte Carlo code," *Med. Phys.* **30**, 179–189 (2003).

<sup>20</sup> G. X. Ding and J. Cygler, "Measurement of  $P_{\text{repl}}P_{\text{wall}}$  factors in electron beams and in a  $^{60}\text{Co}$  beam for plane-parallel chambers," *Med. Phys.* **25**, 1453–1457 (1998).

<sup>21</sup> K. J. Stewart and J. P. Seuntjens, "Comparing calibration methods of electron beams using plane-parallel chambers with absorbed-dose to water based protocols," *Med. Phys.* **29**, 284–289 (2002).

<sup>22</sup> D. W. O. Rogers, "Calibration of parallel-plate ion chambers: Resolution of several problems by using Monte Carlo calculations," *Med. Phys.* **19**, 889–899 (1992).

<sup>23</sup> I. Kawrakow, "Accurate condensed history Monte Carlo simulation of electron transport. I. EGSnrc, the new version," *Med. Phys.* **27**, 485–498 (2000).

<sup>24</sup> I. Kawrakow and D. W. O. Rogers, "The EGSnrc Code System: Monte Carlo simulation of electron and photon transport," Technical Report PIRS-701 (National Research Council of Canada, Ottawa, Canada, 2000) (see <http://www.irs.inms.nrc.ca/inms/irs/EGSnrc/EGSnrc.html>).

<sup>25</sup> I. Kawrakow, "Accurate condensed history Monte Carlo simulation of electron transport. II. Application to ion chamber response simulations," *Med. Phys.* **27**, 499–513 (2000).

<sup>26</sup> J. P. Seuntjens, I. Kawrakow, J. Borg, F. Hobeila, and D. W. O. Rogers,

- “Calculated and measured air-kerma response of ionization chambers in low and medium energy photon beams,” in *Recent Developments in Accurate Radiation Dosimetry, Proceedings of an International Workshop*, edited by J. P. Seuntjens and P. Mobit (Medical Physics Publishing, Madison, WI, 2002), pp. 69–84.
- <sup>27</sup>L. A. Buckley, I. Kawrakow, and D. W. O. Rogers, “CSnrc: Correlated sampling Monte Carlo calculations using EGSnrc,” *Med. Phys.* **31**, 3425–3435 (2004).
- <sup>28</sup>P. R. Almond, F. H. Attix, S. Goetsch, L. J. Humphries, H. Kubo, R. Nath, and D. W. O. Rogers, “The calibration and use of plane-parallel ionization chambers for dosimetry of electron beams: An extension of the 1983 AAPM protocol, Report of AAPM Radiation Therapy Committee Task Group39,” *Med. Phys.* **21**, 1251–1260 (1994).
- <sup>29</sup>D. W. O. Rogers, “Fundamentals of dosimetry based on absorbed-dose standards,” in *Teletherapy Physics, Present and Future*, edited by J. R. Palta and T. R. Mackie (AAPM, Washington DC, 1996), pp. 319–356.
- <sup>30</sup>D. W. O. Rogers, “A new approach to electron beam reference dosimetry,” *Med. Phys.* **25**, 310–320 (1998).
- <sup>31</sup>D. W. O. Rogers, I. Kawrakow, J. P. Seuntjens, and B. R. B. Walters, “NRC User Codes for EGSnrc,” *Technical Report PIRS-702* (National Research Council of Canada, Ottawa, Canada, 2000).
- <sup>32</sup>I. Kawrakow and M. Fippel, “Investigation of variance reduction techniques for Monte Carlo photon dose calculation using XVMC,” *Phys. Med. Biol.* **45**, 2163–2184 (2000).
- <sup>33</sup>G. Mora, A. Maio, and D. W. O. Rogers, “Monte Carlo simulation of a typical <sup>60</sup>Co therapy source,” *Med. Phys.* **26**, 2494–2502 (1999).
- <sup>34</sup>D. Sheikh-Bagheri and D. W. O. Rogers, “Calculation of nine megavoltage photon beam spectra using the BEAM Monte Carlo code,” *Med. Phys.* **29**, 391–402 (2002).
- <sup>35</sup>G. X. Ding and D. W. O. Rogers, “Energy spectra, angular spread, and dose distributions of electron beams from various accelerators used in radiotherapy,” National Research Council of Canada Report PIRS-0439 (see <http://www.irs.inms.nrc.ca/inms/irs/papers/PIRS439/pirs439.html>) (1995).
- <sup>36</sup>C.-M. Ma and A. E. Nahum, “Plane-parallel chambers in electron beams: Monte Carlo findings on perturbation correction factor,” in *Proceedings of the IAEA International Symposium on measurement assurance in dosimetry* (IAEA, Vienna, 1994), pp. 481–493.
- <sup>37</sup>N. I. Kalach and D. W. O. Rogers, “When is an accelerator photon beam ‘cliniclike’ for reference dosimetry purposes,” *Med. Phys.* **30**, 1546–1555 (2003).
- <sup>38</sup>See EPAPS Document No. E-MPHYA6-33-029606 for additional figures showing the wall correction factor in high energy electron beams. This document can be reached via a direct link in the online article’s HTML reference section or via the EPAPS homepage (<http://www.aip.org/pubservs/epaps.html>).